



Original Articles

Repositioning of mifepristone as an integrated stress response activator to potentiate cisplatin efficacy in non-small cell lung cancer



Jirapat Namkaew ^{a,c}, Jun Zhang ^{a,c}, Norio Yamakawa ^{a,c}, Yoshimasa Hamada ^{a,b}, Kazue Tsugawa ^a, Miho Oyadomari ^a, Masato Miyake ^{a,b}, Toyomasa Katagiri ^{d,e}, Seiichi Oyadomari ^{a,b,c,*}

^a Division of Molecular Biology, Institute of Advanced Medical Sciences, Tokushima University, Tokushima, 770-8503, Japan

^b Fujii Memorial Institute of Medical Sciences, Institute of Advanced Medical Sciences, Tokushima University, Tokushima, 770-8503, Japan

^c ER Stress Research Institute Inc., Tokushima, 770-8503, Japan

^d Division of Genome Medicine, Institute of Advanced Medical Sciences, Tokushima University, Tokushima, 770-8503, Japan

^e Laboratory of Biofunctional Molecular Medicine, Center for Drug Design Research, National Institute of Biomedical Innovation, Health and Nutrition, Osaka, 567-0085, Japan

ARTICLE INFO

ABSTRACT

Keywords:

Non-small cell lung cancer (NSCLC)

Integrated stress response (ISR)

Chemosensitization

Mifepristone

Cisplatin

Lung cancer, primarily non-small-cell lung cancer (NSCLC), is a significant cause of cancer-related mortality worldwide. Cisplatin-based chemotherapy is a standard treatment for NSCLC; however, its effectiveness is often limited due to the development of resistance, leading to NSCLC recurrence. Thus, the identification of effective chemosensitizers for cisplatin is of paramount importance. The integrated stress response (ISR), activated by various cellular stresses and mediated by eIF2 α kinases, has been implicated in drug sensitivity. ISR activation globally suppresses protein synthesis while selectively promoting the translation of ATF4 mRNA, which can induce pro-apoptotic proteins such as CHOP, ATF3, and TRIB3. To expedite and economize the development of chemosensitizers for cisplatin treatment in NSCLC, we employed a strategy to screen an FDA-approved drug library for ISR activators. In this study, we identified mifepristone as a potent ISR activator. Mifepristone activated the HRI/eIF2 α /ATF4 axis, leading to the induction of pro-apoptotic factors, independent of its known role as a synthetic steroid. Our *in vitro* and *in vivo* models demonstrated mifepristone's potential to inhibit NSCLC proliferation following cisplatin treatment and tumor growth, respectively, via the ISR-mediated cell death pathway. These findings suggest that mifepristone, as an ISR activator, could enhance the efficacy of cisplatin-based therapy for NSCLC, highlighting the potential of drug repositioning in the search for effective chemosensitizers.

1. Introduction

Lung cancer is the leading cause of cancer-associated deaths worldwide [1], and approximately 85 % of all cases of lung cancer are characterized as non-small-cell lung cancer (NSCLC) [2]. Cisplatin-based chemotherapy is one of the most commonly used chemotherapeutic agents in the clinical treatment of NSCLC [3,4]. Unfortunately, current cisplatin-based treatments for advanced NSCLC result in only modest responses [5,6]. Development of resistance to cisplatin is considered a primary factor in NSCLC recurrence and remains a major clinical problem in the treatment of NSCLC. One of the strategies for inhibiting NSCLC recurrence and prolong survival is to discover an effective

chemosensitizer for cisplatin.

The integrated stress response (ISR) is triggered by cellular stresses, including endoplasmic reticulum (ER) stress, nutrient deprivation, virus infection and hypoxia, all of which can be sensed by four distinct eukaryotic initiation factor 2 alpha (eIF2 α) kinases such as PERK, GCN2, PKR and HRI [7]. Phosphorylation of eIF2 α not only instigates a global suppression of protein synthesis, but also selectively promotes the translation of activating transcription factor 4 (ATF4) mRNA. Specifically, under normal conditions, uORFs in the ATF4 mRNA typically inhibit its translation [8,9]. However, under stress, eIF2 α is phosphorylated, reducing general translation but enhancing ATF4 translation by allowing ribosomes to bypass uORFs and reach the ATF4 start codon [8,

* Corresponding author. Division of Molecular Biology, Institute of Advanced Medical Sciences, Tokushima University, Tokushima, 770-8503, Japan.
E-mail address: oyadomar@tokushima-u.ac.jp (S. Oyadomari).

9]. Thus, ATF4 orchestrates the transcriptional modulation of a wide array of genes [10]. For example, under persistent stress conditions, ATF4 can induce the expression of transcription factors to promote cell death, such as C/EBP homologous protein (CHOP) [11], ATF3 [12] and tribbles pseudokinase 3 (TRIB3) [13]. It was reported that triggering the ISR contributes to drug sensitivity to trastuzumab in HER2+breast cancer cells [14]. Consequently, the identification of cytostatic agents that activate ISR could serve as a therapeutic strategy against cancer.

To reduce time and cost in developing chemosensitizers for the cisplatin treatment of NSCLC, we adopted a strategy to screen an FDA-approved drug library for the ISR activators. Since these repurposed drugs have already passed early stages of drug development, including safety and toxicity studies, they can be swiftly transitioned to clinical trials for their new applications. In this study, we identified that mifepristone as an activator of the ISR. Mifepristone triggered the HRI/eIF2 α /ATF4 axis, leading to the induction of pro-apoptotic factors such as CHOP/DR5/TRIB3, that was independent of its role as a synthetic steroid. Further, we demonstrated the potential of mifepristone to inhibit re-proliferation of NSCLC after cisplatin treatment *in vitro* via ISR-mediated cell death pathway and inhibit NSCLC tumor growth *in vivo*. Our findings indicate that activation of the ISR with mifepristone has potential as a chemosensitizer to cisplatin-based therapy for NSCLC, improving the outcome of therapy.

2. Materials and methods

2.1. Chemicals

Mifepristone (Tokyo Chemical Industry), tolcapone (Cayman Chemical) and BTdCPU (Merck-Millipore) were dissolved in dimethyl sulfoxide (DMSO; FUJIFILM Wako), and progesterone (Tokyo Chemical Industry) was prepared in ethanol (FUJIFILM Wako). All compounds, stored at -30 °C, were freshly diluted in media for each experiment. Cisplatin (FUJIFILM Wako), kept in powder form at 4 °C, was reconstituted in 150 mM NaCl and further diluted in media to yield a final concentration of 100 μM immediately before use. ER stress was elicited by either tunicamycin (Cayman Chemicals) or thapsigargin (Merck-Millipore).

2.2. Cell culture and treatment

The human NSCLC cell lines A549 and HCC4006 kindly provided by Dr. Toyomasa Katagiri (Tokushima University) and Dr. Akira Tangoku (Tokushima University), were respectively cultured in DMEM (Nacalai Tesque) and RPMI-1640 (Nacalai Tesque), both supplemented with 10 % (v/v) fetal bovine serum (FBS; Biosera). The human embryonic kidney (HEK) 293A and HEK293T cell lines were obtained from the American Type Culture Collection (ATCC) and cultured in DMEM supplemented with 10 % (v/v) FBS. Mouse embryonic fibroblasts (MEF) cell line and HEK293A-3xAAARE::Luc2P cells were established as previously described and cultured in DMEM supplemented with 10 % (v/v) FBS [15]. CHO-CHOP::EGFP cells and unphosphorylated eIF2 α mutant (eIF2 α ^{A/A}) cells were kind gifts from Dr. David Ron (University of Cambridge), were respectively cultured in Ham's F-12 (FUJIFILM Wako) and DMEM (Nacalai Tesque), both supplemented with 10 % (v/v) FBS. Cells were cultured at 37 °C in a humidified incubator continuously flushed with a mixture of 5 % CO₂ and 95 % air. All cell lines were routinely PCR-tested for *Mycoplasma*.

2.3. Generation of lentivirus and transduction

Lentiviral particles were produced in HEK293T cells using psPAX2 (Addgene, Plasmid 12260) and pMD2. G (Addgene, Plasmid 12259) packaging plasmids with PEI-MAX transfection reagent (Polysciences). The medium was changed 6–8 h post-transfection and cells were further incubated for 72 h to facilitate virus production. The supernatant,

containing lentiviruses, was harvested, and cleared of cell debris via centrifugation. Target cells were subsequently transduced in the presence of 8 μg/mL hexadimethrine bromide (Polybrene; Sigma-Aldrich). Following overnight transduction, the medium was changed, and cells were further propagated for downstream applications.

2.4. Generation of CRISPR/Cas9-knockout cell lines

The specific single-guide RNA (sgRNA) sequences were selected via the CRISPR Design Tool (<http://crispor.tefor.net>) and cloned into LentiGuide-Puro (Addgene, Plasmid 52963). Cas9 nuclease-expressing HEK293A cells were generated by transduction with lentiviral Cas9 nuclease expression particles, followed by selection with 10 μg/mL blasticidin S (Kaken Pharmaceutical) for 7 days. These cells were subsequently transduced with Lentiviral sgRNA particles and selected with 2 μg/mL puromycin (GoldBio) for 7 days. Knockout cell pools were isolated into 96-well plates for single clonal cell generation, with an empty vector without sgRNA serving as a negative control. The knockout efficacy of promising cell clones was evaluated via DNA sequencing using 3130xl Genetic Analyzers (Applied Biosystems) and protein functionality was confirmed by immunoblotting with corresponding antibodies.

2.5. Generation of doxycycline inducible ATF4 expression cells

A549 cells were transduced with lentiviral Tet3G particles, followed by lentiviral TRE3G particles harboring mouse ATF4-IRES-EGFP. Upon induction with 200 ng/mL doxycycline (Enzo Life Sciences), cells expressing EGFP were sorted using an S3e cell sorter (Bio-Rad), and cells were further propagated for downstream applications.

2.6. Cell proliferation assay and cell death assay

Cells were seeded at a density of 1.5×10^3 cells/well in 96-well plates and cultured overnight. Subsequently, cells were exposed to 100 μM cisplatin for 1 h, followed by a phosphate-buffered saline (PBS) wash. Cells were then treated with either 20 μM of mifepristone or 5 μM BTdCPU or a mock treatment (DMSO) for a period of 22 days, with media changes containing mifepristone every 2 days. Cell viability was periodically assessed using the water-soluble tetrazolium salt-8 (WST-8) assay (Kishida Chemical), following the manufacturer's guidelines. The optical density of each well was measured at 450 nm using an EnVision plate reader (PerkinElmer). Cells were observed and photographed under an inverted fluorescent microscope (IX-70; Olympus) with a phase contrast objective.

Additionally, cell proliferation was assessed using the CyQUANT Direct Cell Proliferation Assay Kit (Invitrogen), in accordance with the manufacturer's guidelines. Subsequently, cells were gently washed twice with PBS and incubated with 5 μg/mL propidium iodide (PI; Sigma-Aldrich) for 5–10 min in darkness. Afterwards, the stained cells were washed twice with PBS, and images were captured using an inverted fluorescent microscope (IX-70; Olympus).

2.7. Quantitative reverse transcription PCR (qRT-PCR) analysis

Total RNA was isolated using TRIzol and followed by isopropanol precipitation. 400 ng of RNA were used as templates for cDNA synthesis with ReverTra Ace qPCR RT Master Mix with gDNA Remover (TOYOBO Life Science) according to the manufacturer's protocol. qRT-PCR was performed using the Step One Plus Real-Time PCR System (Applied Biosystems) with Power SYBR Green PCR Master Mix (Applied Biosystems). The primer sequences were as follows; mouse *Atf4*: 5'-AGGAAGCCTGACTCTGCTGC-3' (forward); 5'-AGGCAGATTGTCTGG TGGGG-3' (reverse), human *ATF4*: 5'-GGTCAGTCCTCCAACAACA-3' (forward); 5'-CTATACCCAACAGGGCATCC-3' (reverse) and 18sRNA: 5'-GTAACCGTTGAACCCCATT-3' (forward); 5'-GATGGTAGTCGC

CGTGCC-3' (reverse).

2.8. Actinomycin D mRNA stability assay

MEF cells were pretreated with 2, 5 and 10 µg/mL actinomycin D (Nacalai Tesque) for 5 min followed by mifepristone (50 µM) treatment for additional 2 h. Total RNA was then extracted using TRIzol, and *Atf4* mRNA expression levels were analyzed via qRT-PCR.

2.9. Immunoblot analysis

Protein lysates were obtained by lysing in RIPA buffer (50 mM Tris pH 7.5, 150 mM NaCl, 1 mM EDTA, 0.1 % SDS, 1 % NP-40, 0.5 % deoxycholic acid) with protease inhibitor cocktail (Nacalai Tesque) and phosphatase inhibitor cocktail (Biotool). Protein lysates (15 µg) were separated by SDS-PAGE and then transferred to nitrocellulose membranes. The membranes were blocked in Blocking One or Blocking One-P (Nacalai Tesque) and then separately probed with the primary antibodies, followed by HRP-conjugated secondary antibodies. The blot was developed using Immobilon Western Chemiluminescent HRP Substrate (Merck-Millipore) and visualized using Ez-Capture II (ATTO Corp) and Amersham ImageQuant 800 system (Cytiva), and the band intensities were quantified using Image Studio software (Li-Cor Biosciences). The sources of antibodies were as follows: anti-phospho-Ser51-eIF2α (D9G8 #3398, Cell Signaling Technology); anti-eIF2α (D7D3 #5324, Cell Signaling Technology); anti-phospho-Thr980-PERK (16F8 #3179, Cell Signaling Technology); anti-ATF4 (D4B8 #11815, Cell Signaling Technology); anti-CHOP (15204-1-AP, Proteintech); anti-ATF3 (SC-518032, Santa cruz); anti-TRIB3 (HPA015272, Sigma-Aldrich); anti-phospho-S724-IKE1 (ab124945, Abcam); anti-XBP1s (D2C1F #12782, Cell Signaling Technology); anti-ATF6 (clone ATZ-09; a gift from Japan Tobacco); anti-KDEL (GRP78) (PM059, MBL); anti-DR5 (D4E9, #8074, Cell Signaling Technology); anti-cleaved-Asp214-PARP (#9544, Cell Signaling Technology); anti-β-Actin (M177-3, MBL); anti-progesterone receptor A/B (D8Q2J #8757, Cell Signaling Technology).

2.10. Cycloheximide protein stability assay

MEF cells were treated with 200 nM thapsigargin for 6 h, after which they were exposed to 100 µM cycloheximide (FUJIFILM Wako Chemical) in the presence of either 20 µM mifepristone or 20 µM MG-132 (Enzo Life Sciences). Cells were collected at 0, 20, 40, 60, and 120 min post-cycloheximide addition, and protein lysates were prepared. ATF4 protein levels were subsequently determined by immunoblotting.

2.11. In vivo mice studies

The experimental protocols involving animals were approved by the Animal Research Committee of Tokushima University, and all experiments were performed in accordance with the appropriate institutional guidelines.

Male nude (**KSN/Slc, SLC, Japan**) mice aged 6–7 weeks were used in the study. A549 cells were transduced with lentiviral EGFP particles, with EGFP-positive cells subsequently sorted using an S3e cell sorter (Bio-Rad). Mice were intravenously injected in the lateral tail vein with $0.6\text{--}1.2 \times 10^6$ A549-EGFP expressing cells suspended in PBS and were randomly assigned to treatment groups. One day post-cell injection, mice received a single subcutaneous dose of cisplatin (5 mg/kg in 150 mM NaCl). Beginning the following day, mice were orally administered mifepristone (20 mg/kg) three times daily for 9 days. Control mice were given a vehicle (0.25 % CMC in water). Body weights of all mice were recorded daily. At the experimental endpoint, mice were euthanized, and their lungs were harvested for analysis. Tumor formation by A549-EGFP cells was observed using a Leica M205 FA fluorescence stereo microscope and tumor nodules were photographed at the same magnification (8X). The area of the EGFP-tumor colonies was quantified using

Image Studio software (Li-Cor Biosciences). The volume of the EGFP-tumor colonies was calculated from the area of the EGFP-tumor colonies by the following equation;

$$\text{Radius} = \sqrt{\frac{\text{Area}}{\pi}}$$

$$\text{Volume} = \frac{4}{3}\pi r^3$$

2.12. Statistical analysis

Data were analyzed using GraphPad Prism 9 (GraphPad Software) and are shown as mean \pm standard error of the mean (SEM) from minimum of three independent experiments. Results were analyzed by Student's *t*-test and one- or two-way ANOVA as indicated in the figure legends and were considered significant at a value of $p < 0.05$ and $p < 0.01$ respectively.

3. Results

3.1. Identification of mifepristone as a potent ISR activator

To identify novel ISR activators, we conducted a combined approach of two cell-based ISR screenings using two distinct reporters in two different cell types. The first screening, we utilized CHO-CHOP::EGFP cells, which report CHOP expression, a downstream gene induced by the ISR, via EGFP [16]. The second screening, we employed HEK293A-3x-AARE::Luc2P cells, which report AARE activity, the binding site for ATF4, via Luc2P [15]. Screening of 1,271 FDA-approved compounds from the Prestwick Chemical Library yielded three hits: mifepristone, progesterone, and tolcapone (Fig. 1A). Hit validation was conducted through immunoblot analysis of ATF4 protein, a central player in the ISR-induced transcriptional program. While all hit compounds induced ATF4, mifepristone induced it at a lower concentration and with stronger expression induction in HEK293A cells (Fig. 1B). Therefore, present research was focused on mifepristone (Fig. 1C). Additionally, we confirmed the dose-dependency and time course of the ATF4 protein induction by mifepristone in MEF cells (Fig. 1D and E). Collectively, these findings demonstrate that mifepristone activates the ISR.

3.2. ISR activation by mifepristone is independent of its function as a synthetic steroid hormone

ATF4, a key mediator of the ISR, is primarily regulated at the translational level, although induction at the transcriptional level has also been reported [17]. To elucidate the mechanism of ISR activation by mifepristone, we first investigated whether ATF4 mRNA is induced by mifepristone using RT-qPCR. We found that ATF4 mRNA increased in a dose-dependent manner with mifepristone (Fig. 2A) and reached near-maximum levels within 2 h of mifepristone addition (Fig. 2B). Given the instability of ATF4 mRNA, we considered the possibility that its increase could be due to mRNA stabilization. However, when transcription was inhibited using the RNA synthesis inhibitor actinomycin D, mifepristone-induced ATF4 mRNA was almost completely abolished (Fig. 2C), suggesting that transcriptional induction is necessary for the increase in ATF4 mRNA by mifepristone.

Mifepristone was originally developed as a synthetic steroid hormone, acting as a highly active antagonist of both the progesterone receptor (PR) and the glucocorticoid receptor (GR). PR and GR can bind to progesterone response elements (PRE) and glucocorticoid response elements (GRE) in the promoter region, respectively, activating or repressing the transcription of target genes. Therefore, we searched for the PRE and GRE in the genomic region upstream of ATF4 gene using Genomatix Gene2Promoter software. Our *in-silico* search did not identify any GREs, but we did find the putative PRE at positions –1067 and

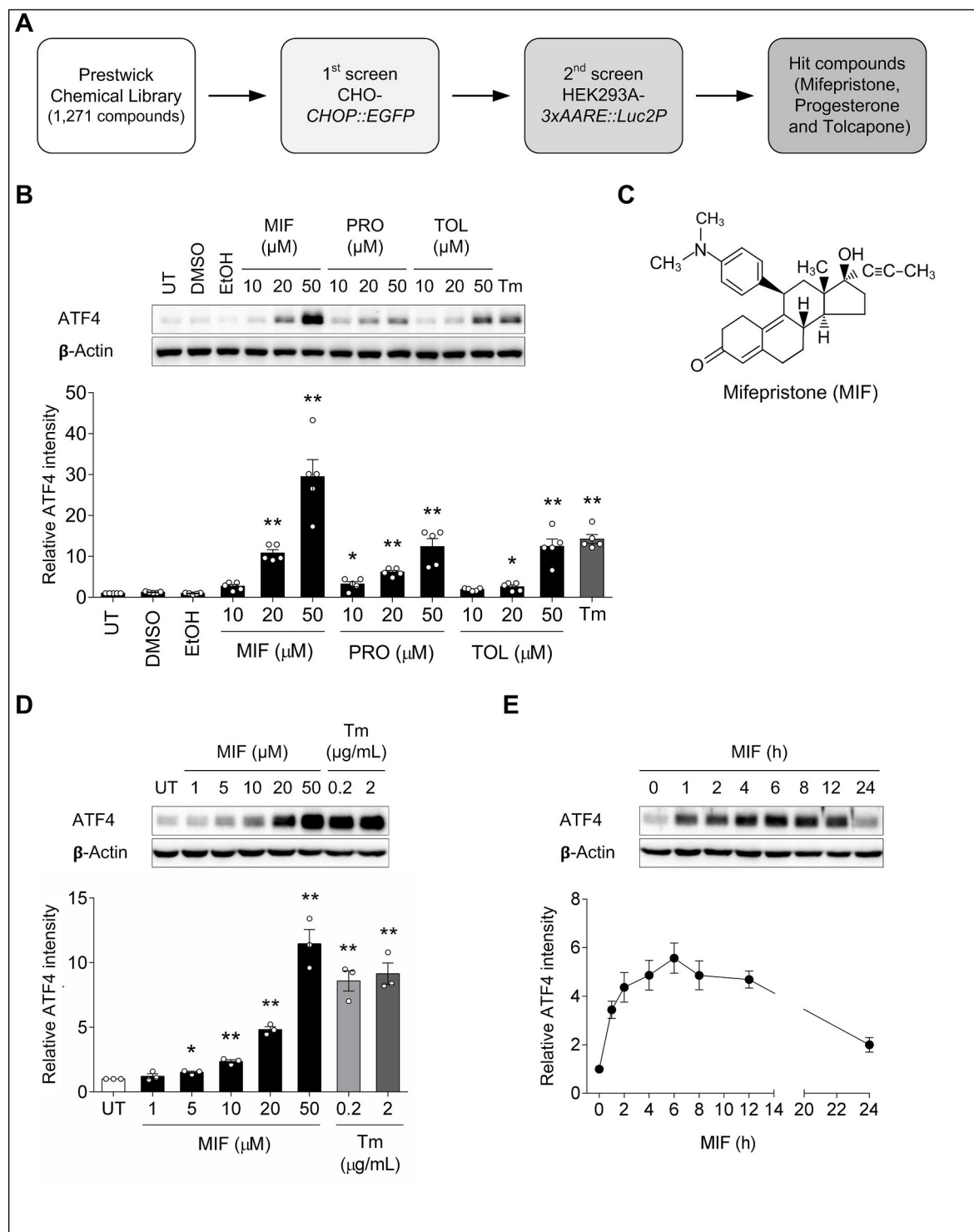


Fig. 1. Identification of mifepristone as a potent ISR activator.

(A) Schematic representation of the screening protocol for ISR activator identification. (B) Representative immunoblots and quantification of ATF4 in HEK293A cells 6 h after varying concentrations of mifepristone (MIF), progesterone (PRO), and tolcapone (TOL). Tunicamycin (Tm; 2 $\mu\text{g/mL}$) served as a positive control. Data are means \pm SEMs ($n = 5$). Statistical analysis was performed using Student's t-test, * $p < 0.05$, ** $p < 0.01$ compared to mock (DMSO or EtOH) treated cells. (C) Chemical structure of mifepristone. (D) Representative immunoblots and quantification of ATF4 in MEF cells treated with indicated concentrations of mifepristone (MIF) for 6 h. Data are means \pm SEMs ($n = 3$). Statistical analysis was performed using Student's t-test, ** $p < 0.01$ compared to untreated cells (UT). (E) Representative immunoblots and quantification of ATF4 in MEF cells treated with 20 μM mifepristone for the indicated time periods. Data are means \pm SEMs ($n = 3$).

–1048 bp from the transcription start site (Fig. 2D), suggesting the possibility of mifepristone-induced ATF4 mRNA via PR-PRE. To test this hypothesis, we introduced mutations into Exon3, common to both PR isoforms PR-A and PR-B, to create PR knockout (PR-KO) cells (Fig. 2E and Supplementary Fig. S1). However, we observed no difference in

mifepristone-induced ATF4 mRNA between wild-type and PR-KO cells (Fig. 2F). Overall, these results suggest that the function of mifepristone as a synthetic steroid hormone does not contribute to its activation of the ISR.

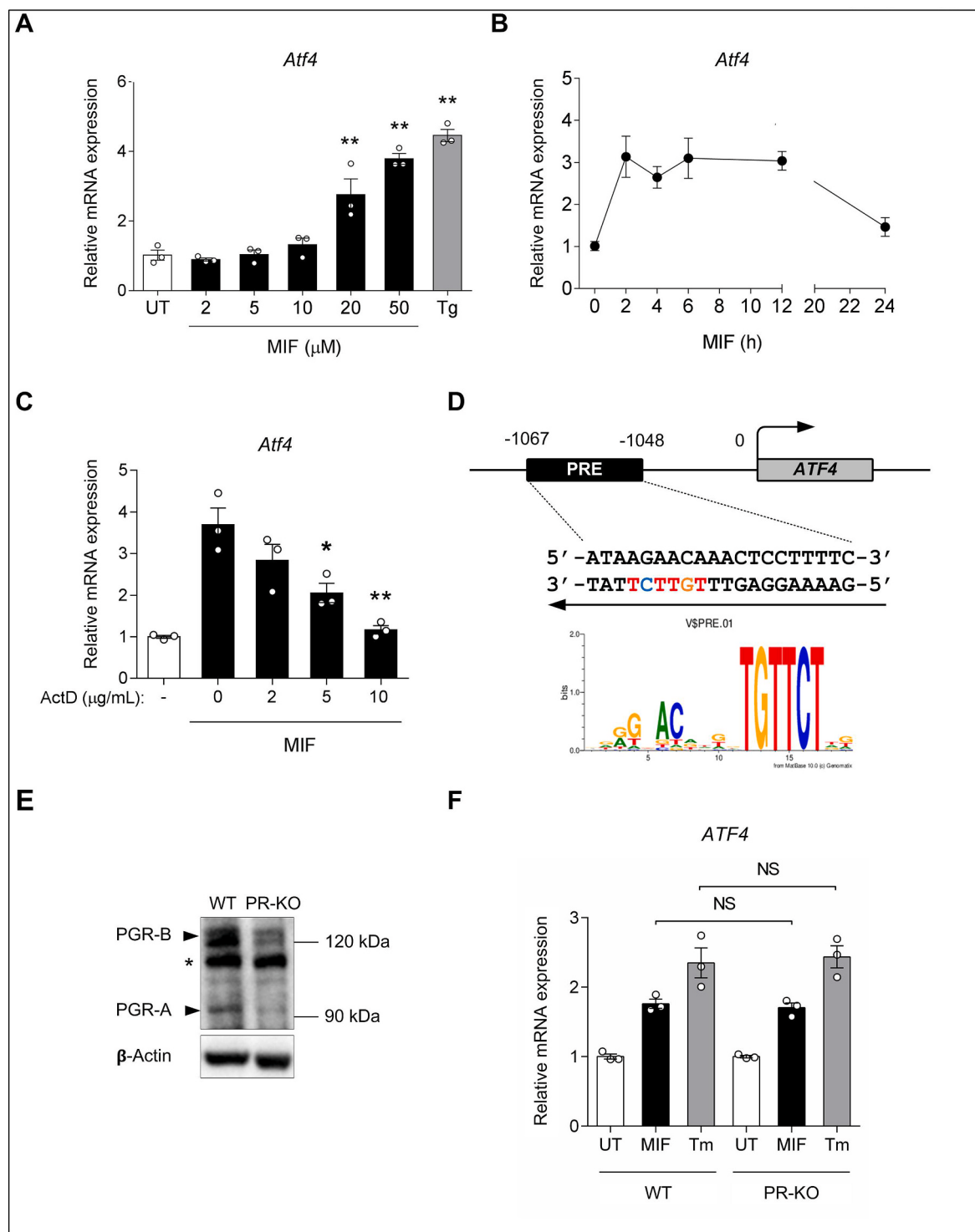


Fig. 2. Mifepristone-induced ATF4 is independent of its function as a synthetic steroid hormone.

(A) qRT-PCR analysis of *Atf4* mRNA levels in MEF cells treated with indicated concentrations of mifepristone (MIF) for 6 h. Thapsigargin (Tg; 200 nM) served as a positive control. Data are means \pm SEMs ($n = 3$). Statistical analysis was performed using Student's *t*-test, ** $p < 0.01$ compared to untreated cells (UT). (B) qRT-PCR analysis of *Atf4* mRNA levels in MEF cells treated with 20 μM mifepristone (MIF) for the indicated time periods. Data are means \pm SEMs ($n = 3$). (C) Actinomycin D mRNA stability assays. qRT-PCR analysis of *Atf4* mRNA levels in MEF cells pretreated with indicated concentrations of actinomycin D (ActD) for 5 min followed by 20 μM mifepristone (MIF) treatment for an additional 2 h. Data are means \pm SEMs ($n = 3$). Statistical analysis was performed using Student's *t*-test, * $p < 0.05$, ** $p < 0.01$ compared to ActD 0 $\mu\text{g/mL}$ (MIF treatment alone). (D) Schematic representation of the promoter region of *ATF4*, containing progesterone receptor responsive element (PRE). The sequence logo of PRE from Gene2Promoter analysis showing the information content of the base frequency at that position. (E) Representative immunoblots of progesterone receptor (PGR) isoforms A and B in HEK293A wild type (WT) and progesterone receptor knockout (PR-KO) cells. *, non-specific band. Data are representative of three reproducible and independent experiments. (F) qRT-PCR analysis of *ATF4* mRNA levels in HEK293A WT and PR-KO cells treated with 20 μM mifepristone (MIF) for 6 h. Tunicamycin (Tm; 2 $\mu\text{g/mL}$) served as a positive. Data are presented as mean \pm SEM ($n = 3$). Statistical analysis was performed by Student's *t*-test, NS = not significant ($p > 0.05$) compared to WT of each treatment.

3.3. ISR activation by mifepristone is mainly regulated by HRI-eIF2 α signaling axis

It is well documented that ATF4 expression is predominantly regulated at the translational level, a process governed by upstream open

reading frames (uORFs) within its mRNA. The phosphorylation of eIF2 α at serine 51 facilitates the bypass of inhibitory ATF4 uORFs, thereby enabling the translation of the ATF4 coding sequence [8,9]. Therefore, we sought to evaluate the necessity of eIF2 α phosphorylation in mifepristone-induced ATF4 expression. To this end, we treated MEF

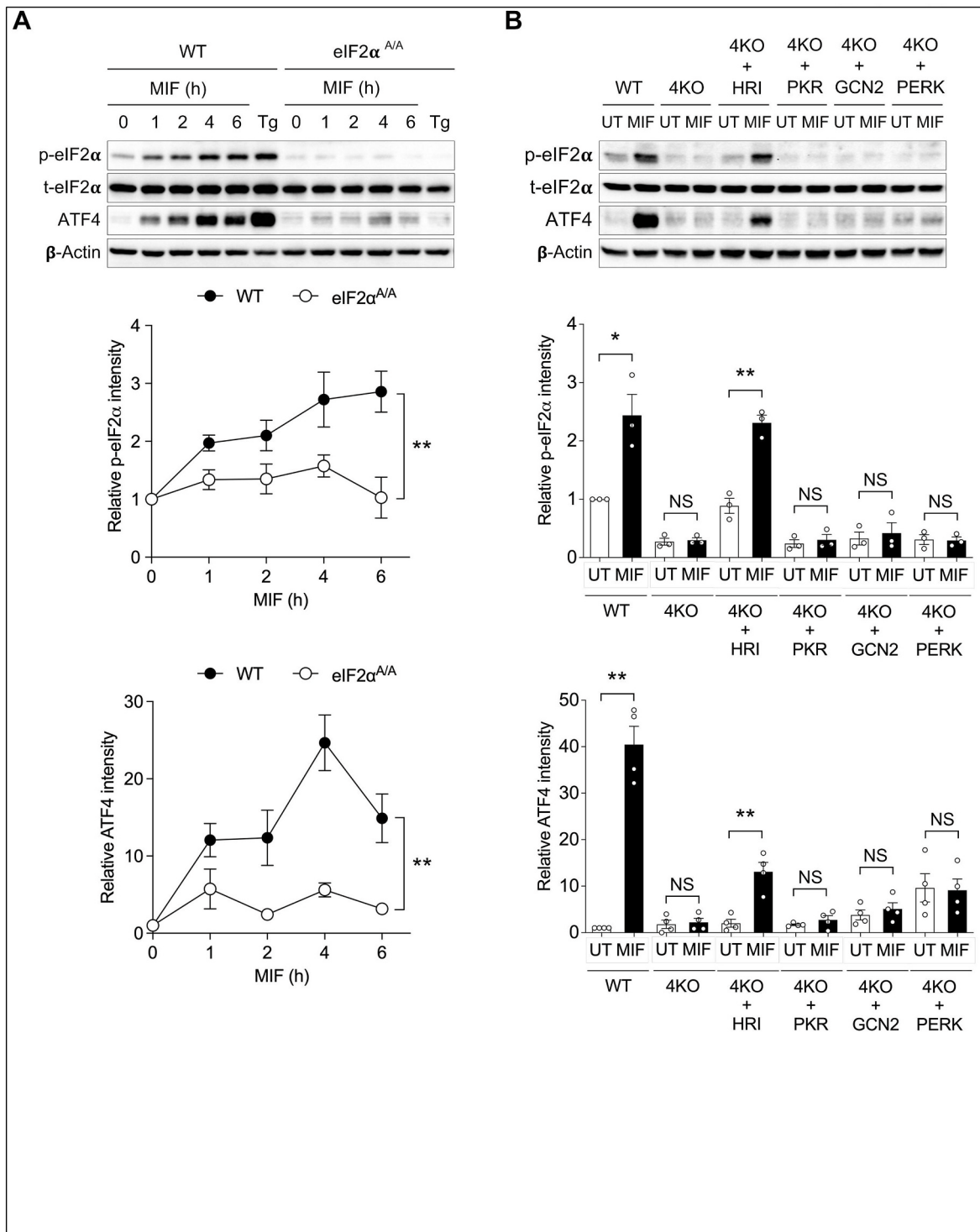


Fig. 3. Mifepristone-induced ATF4 expression is mainly regulated by phosphorylated eIF2 α .

(A) Representative immunoblots and quantification of phosphorylated eIF2 α (p-eIF2 α) and ATF4 in MEF wild type (WT) and unphosphorylated eIF2 α mutant (eIF2 α ^{AA}) cells treated with 20 μ M mifepristone (MIF) for the indicated time periods ($n = 3$). Thapsigargin (Tg; 200 nM) was served as a positive control. Statistical analysis was performed by two-way ANOVA, * $p < 0.05$, ** $p < 0.01$ compared to 0 h. (B) Representative immunoblots and quantification of phosphorylated eIF2 α and ATF4 in MEF cells with all four known eIF2 α kinases deleted (4KO), and in 4KO cells where a single eIF2 α kinase was reintroduced. Cells were treated with 20 μ M mifepristone (MIF) for 2 h ($n = 3-4$). Statistical analysis was performed by Student's *t*-test, * $p < 0.05$, ** $p < 0.01$ compared to UT.

cells, in which eIF2 α had been mutated at serine 51 to a non-phosphorylatable alanine (eIF2 $\alpha^{A/A}$), with mifepristone. Mifepristone-induced ATF4 expression was largely inhibited in eIF2 $\alpha^{A/A}$ MEF cells, indicating that mifepristone-induced ATF4 expression is highly dependent on eIF2 α phosphorylation (Fig. 3A).

Given that post-translational regulation, including ATF4 protein

stability, is known to influence ATF4 expression [10,18], we further conducted a cycloheximide protein stability assay. Although the proteasome inhibitor MG132 stabilized ATF4, mifepristone treatment did not impact ATF4 stability compared to the control. These results suggest that mifepristone does not increase ATF4 protein by inhibiting its rapid turnover (Supplementary Fig. S3).

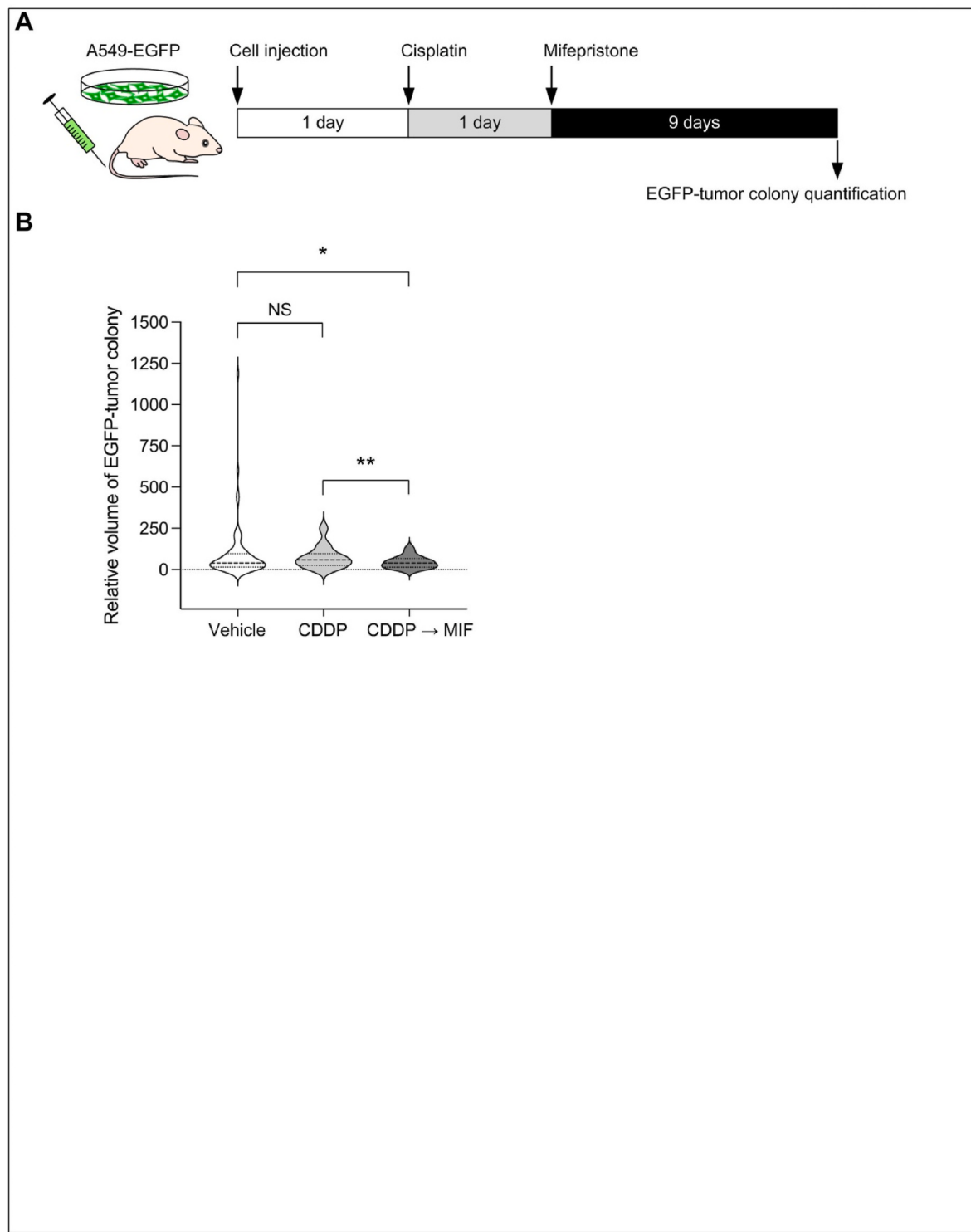


Fig. 4. *In vivo* anti-tumor activity of mifepristone after cisplatin treatment.

(A) Schematic representation of *in vivo* treatment strategy. (B) Quantification of the volume of A549 EGFP-tumor colonies in the lungs of male nude mice treated with vehicle ($n = 59$ colonies from 9 mice) and with 5 mg/kg cisplatin (CDDP) followed by vehicle ($n = 49$ colonies from 10 mice) or 3 doses of 20 mg/kg mifepristone (MIF) per day ($n = 39$ from 10 mice) for 9 days. After treatment, lungs were collected to quantify the EGFP-tumor colonies under an inverted fluorescent microscope. Statistical analysis was performed by Student's *t*-test, ** $p < 0.01$, * $p < 0.05$ and NS = not significant.

To identify the eIF2 α kinase responsible for the response to mifepristone, we took advantage of our previously established quadruple knockout (4KO) cells, devoid of all four known eIF2 α kinases (PKR, GCN2, HRI, and PERK), and single eIF2 α kinase-rescued 4KO cell lines [19]. As anticipated, mifepristone-induced eIF2 α phosphorylation and ATF4 induction were entirely abolished in the 4KO cells (Fig. 3B).

Importantly, we found that only HRI rescue could mediate mifepristone-induced phospho-eIF2 α and ATF4, indicating that HRI, among the eIF2 α kinases, is responsible for mifepristone-induced ATF4 expression (Fig. 3B). Furthermore, we confirmed that the upregulation of eIF2 α and ATF4, induced by mifepristone, was significantly attenuated in HRI single-knockout MEF cells. This provides evidence for HRI's

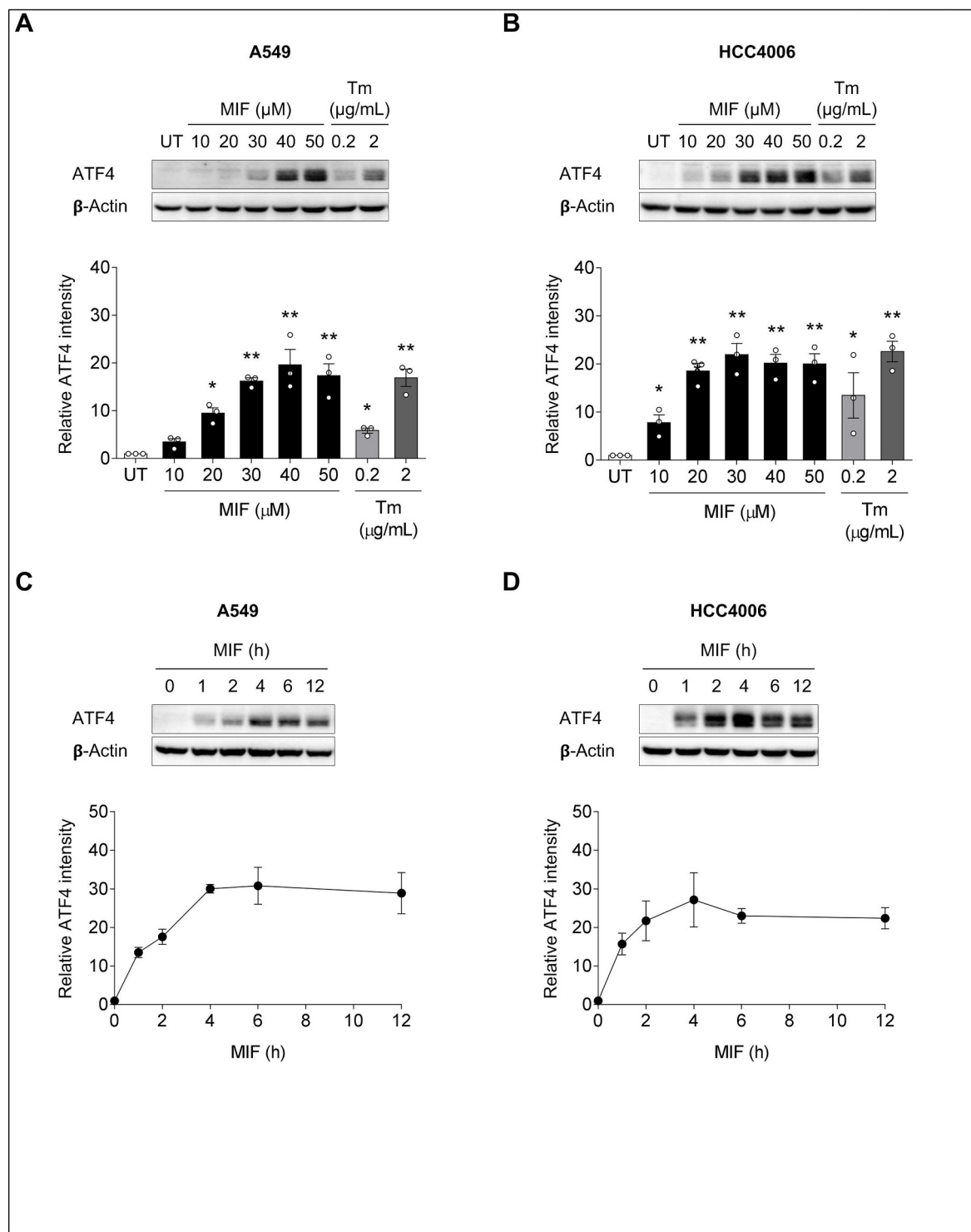


Fig. 5. Mifepristone induces ATF4 expression in dose- and time-dependent manner in human NSCLC cell lines.

(A) Representative immunoblots and quantification of ATF4 in A549 and (B) HCC4006 cells treated with indicated concentrations of mifepristone (MIF) for 6 h. Tunicamycin (Tm; 0.2 and 2 μ g/mL) served as a positive control. Data are means \pm SEMs ($n = 3$). Statistical analysis was performed by Student's *t*-test, * $p < 0.05$, ** $p < 0.01$ compared to untreated cells (UT). (C) Representative immunoblots and quantification of ATF4 in A549 and (D) HCC4006 cells treated with 20 μ M mifepristone (MIF) for the indicated time periods. Data are means \pm SEMs ($n = 3$).

role as the eIF2 α kinase responsible for mifepristone-induced ISR activation (Supplementary Fig. S2). Collectively, these results indicate that mifepristone primarily promotes ATF4 increase through translational control via the HRI-eIF2 α signaling axis.

3.4. Mifepristone enhances cisplatin sensitivity and inhibits non-small cell lung cancer tumor growth *in vivo* mice model

To evaluate the potential of mifepristone as a chemosensitizer that induces synthetic lethality and enhances the sensitivity of NSCLC to cisplatin, we established a lung tumor model by inoculating the human NSCLC cell line A549 cells via tail vein injection. A549 cells were labeled with EGFP for sensitive and quantitative assessment of tumor colonies via fluorescence signal. Following cisplatin administration, mice were treated with mifepristone, and pulmonary tumor growth was analyzed as described in the methods section (Fig. 4A). Notably, eleven days post A549-EGFP cell inoculation and treatment, the EGFP signal was detectable in both groups. Mifepristone treatment significantly reduced the volume of EGFP-tumor colonies compared to the vehicle-treated and cisplatin-treated groups, from 100.00 ± 23.86 colonies to 44.26 ± 5.71 colonies (2.26-fold) and from 74.83 ± 9.55 colonies to 44.26 ± 5.71 colonies (1.69-fold), respectively (Fig. 4B). Collectively, these findings demonstrate mifepristone's capacity to enhance cisplatin sensitivity and inhibit NSCLC tumor growth.

3.5. Mifepristone increases ATF4 expression in two NSCLC cell lines with distinct genetic backgrounds

Given the observed *in vivo* efficacy of mifepristone as a chemosensitizer for cisplatin, we decided to elucidate its molecular mechanism using NSCLC cell lines. In NSCLC, a variety of genetic mutations significantly influence disease onset, progression, and treatment response. Among these, KRAS and EGFR mutations are the most prevalent. Thus, we selected to use A549 cells, which have a KRAS-mutant genetic background, and HCC4006 cells, which have an EGFR-mutant genetic background, for further analysis. Initially, we verified whether mifepristone could induce ATF4 in A549 and HCC4006 cells. As anticipated, our immunoblot analysis confirmed that mifepristone induced ATF4 in both A549 and HCC4006 cell lines, which have distinct genetic backgrounds, in a dose- and time-dependent manner (Fig. 5A–D). This is consistent with our results using MEF or HEK293A cells, indicating that mifepristone can induce ATF4 in NSCLC cells regardless of their specific genetic backgrounds.

3.6. Mifepristone inhibits re-proliferation of NSCLC cells *in vitro* following cisplatin treatment

Upon observing the *in vivo* efficacy of mifepristone as a chemosensitizer for cisplatin, we aimed to elucidate its molecular mechanism using NSCLC cell lines *in vitro*. Initially, we evaluated the inhibitory effects of mifepristone on A549 and HCC4006 cell proliferation (Fig. 6A). After 22 days of treatment, mifepristone concentrations exceeding $20 \mu\text{M}$ completely inhibited cell proliferation in both cell lines (Fig. 6B). To recapitulate the chemosensitizing effects of mifepristone *in vitro*, we utilized a concentration of $20 \mu\text{M}$ mifepristone in subsequent experiments. This concentration did not significantly alter the viability of HCC4006 cells and maintained the viability of A549 cells above 80% (Fig. 6B).

We then established a long-term *in vitro* model of tumor cell re-proliferation to mimic the recurrence of NSCLC observed *in vivo* (Fig. 6C). Following a 1-h cisplatin treatment and a subsequent medium change to include mifepristone, we assessed cell morphology and proliferation after 22 days. Post-cisplatin treatment, both A549 and HCC4006 cells exhibited a higher proportion of spindle-like or round-shaped cells, indicative of not only inhibited cell proliferation but also cell death (Fig. 6D and Supplementary Fig. S4). Indeed, we observed that

mifepristone significantly inhibited the re-proliferation of both A549 and HCC4006 cells following cisplatin treatment (Fig. 6E). Thus, we were able to confirm the chemosensitizing effects of mifepristone *in vitro* using NSCLC cells.

3.7. Activation of the HRI/eIF2 α /ATF4 axis inhibits NSCLC re-proliferation after cisplatin treatment

Given that we demonstrated mifepristone activates the ISR via HRI activation in Fig. 3, we sought to determine the contribution of HRI-mediated ISR activation to mifepristone's role as a chemosensitizer for cisplatin. To this end, we tested whether BTdCPU, a known HRI activator [20], could function as a chemosensitizer for cisplatin in our *in vitro* model of tumor cell re-proliferation (Fig. 7A). BTdCPU was identified as a selective HRI activator through a compound library screening that used ATF4 mRNA translation as a readout [20]. Indeed, in both A549 and HCC4006 cells used in our *in vitro* model of tumor cell re-proliferation, we confirmed that BTdCPU increased ATF4 protein levels to a similar extent as mifepristone (Fig. 7B and Supplementary Fig. S5). Like mifepristone, BTdCPU induced morphological changes indicative of cell death, such as spindle-like or round-shaped cells, in both A549 and HCC4006 cells following cisplatin treatment (Fig. 7C). Subsequent analysis using the CyQUANT Direct Assay confirmed these cells to be non-viable (Supplementary Fig. S4). Furthermore, BTdCPU, like mifepristone, inhibited the re-proliferation of both A549 and HCC4006 cells following cisplatin treatment (Fig. 7D). Consistent with these findings, we observed induction of CHOP, a known apoptosis marker in the ISR, in both A549 and HCC4006 cells on day 1 and day 7 following cisplatin treatment and subsequent administration of either BTdCPU or mifepristone (Fig. 7B).

We further investigated the contribution of ISR activation to the chemosensitizing effect of cisplatin using a genetic approach. For this purpose, we established A549 cells (A549-TetON::mATF4 cells) capable of inducing ATF4 upon doxycycline treatment using lentiviral transduction (Supplementary Figs. S6A and B). We then examined whether the induction of ATF4 alone, without HRI or eIF2 α phosphorylation, could result in chemosensitization for cisplatin in our *in vitro* model of tumor cell re-proliferation using A549-TetON::mATF4 cells (Supplementary Fig. S6C). Contrary to the effect of cisplatin pretreatment alone, overexpression of mATF4 induced by doxycycline treatment led to a significant reduction in cell re-proliferation (Supplementary Fig. S6D). These results demonstrate that the activation of the ISR via the HRI/eIF2 α /ATF4 axis inhibits NSCLC re-proliferation following cisplatin treatment.

3.8. Mifepristone inhibits NSCLC re-proliferation after cisplatin treatment through ISR-mediated cell death

Mifepristone's role as an activator of the integrated stress response (ISR) is not only associated with tumor growth inhibition but also appears to induce cell death, as suggested by observed morphological changes shown in Figs. 6D and 7C. To confirm whether this cell death was due to apoptosis, we examined the expression of cleaved poly (ADP-ribose) polymerase (Cl-PARP), an apoptosis marker, by immunoblot analysis. In both A549 and HCC4006 cells, mifepristone enhanced the cisplatin-induced increase in Cl-PARP, suggesting the induction of apoptosis (Fig. 8F and Supplementary Fig. S7).

Apoptosis is a tightly regulated process overlapping multiple pathways. In the context of ISR, these pathways converge on mitochondria, forming the intrinsic pathway, and also involve receptor-mediated processes, known as the extrinsic pathway. We first examined the induction of CHOP, a pro-apoptotic factor inducer, which contributes to the intrinsic pathway of apoptosis. Mifepristone enhanced the cisplatin-induced increase in CHOP in both A549 and HCC4006 cells (Fig. 8C and Supplementary Fig. S7). Additionally, the intrinsic pathway can be indirectly activated by suppressing survival signals, such as those

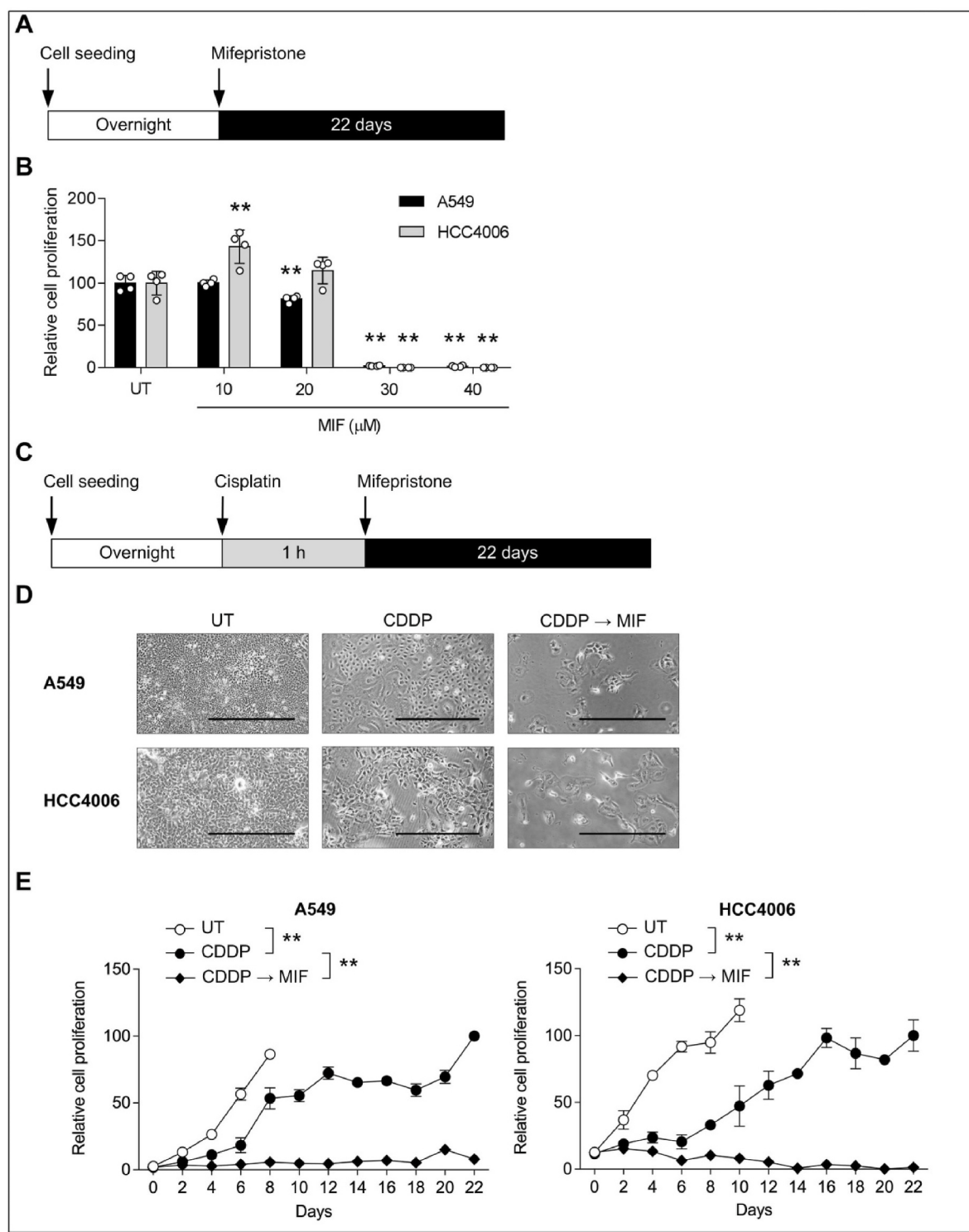


Fig. 6. Mifepristone inhibits re-proliferation of NSCLC cells *in vitro* following cisplatin treatment.

(A) Schematic representation of treatment strategy of mifepristone. (B) Relative cell proliferation of A549 and HCC4006 cells determined by WST-8 assay. Both cells were treated with the indicated concentrations of mifepristone (MIF) for 22 days. Data are means \pm SEMs ($n = 4$). Statistical analysis was performed by Student's *t*-test, $*p < 0.05$, $**p < 0.01$ compared to untreated cells (UT). Data are representative of three reproducible and independent experiments. (C) Schematic representation of NSCLC re-proliferation assay. (D) Representative microscopic images of A549 and HCC4006 cells treated with cisplatin only or cisplatin followed by mifepristone for 8 days. Scale bars, 500 μ M. (E) Relative cell proliferation of A549 and HCC4006 cells determined by WST-8 assay. The indicated cells were pre-treated with 100 μ M cisplatin (CDDP) for 1 h followed by 20 μ M mifepristone (MIF) for 22 days. Data are means \pm SEMs ($n = 4-6$). Statistical analysis was performed by two-ANOVA, $**p < 0.01$. Data are representative of four reproducible and independent experiments.

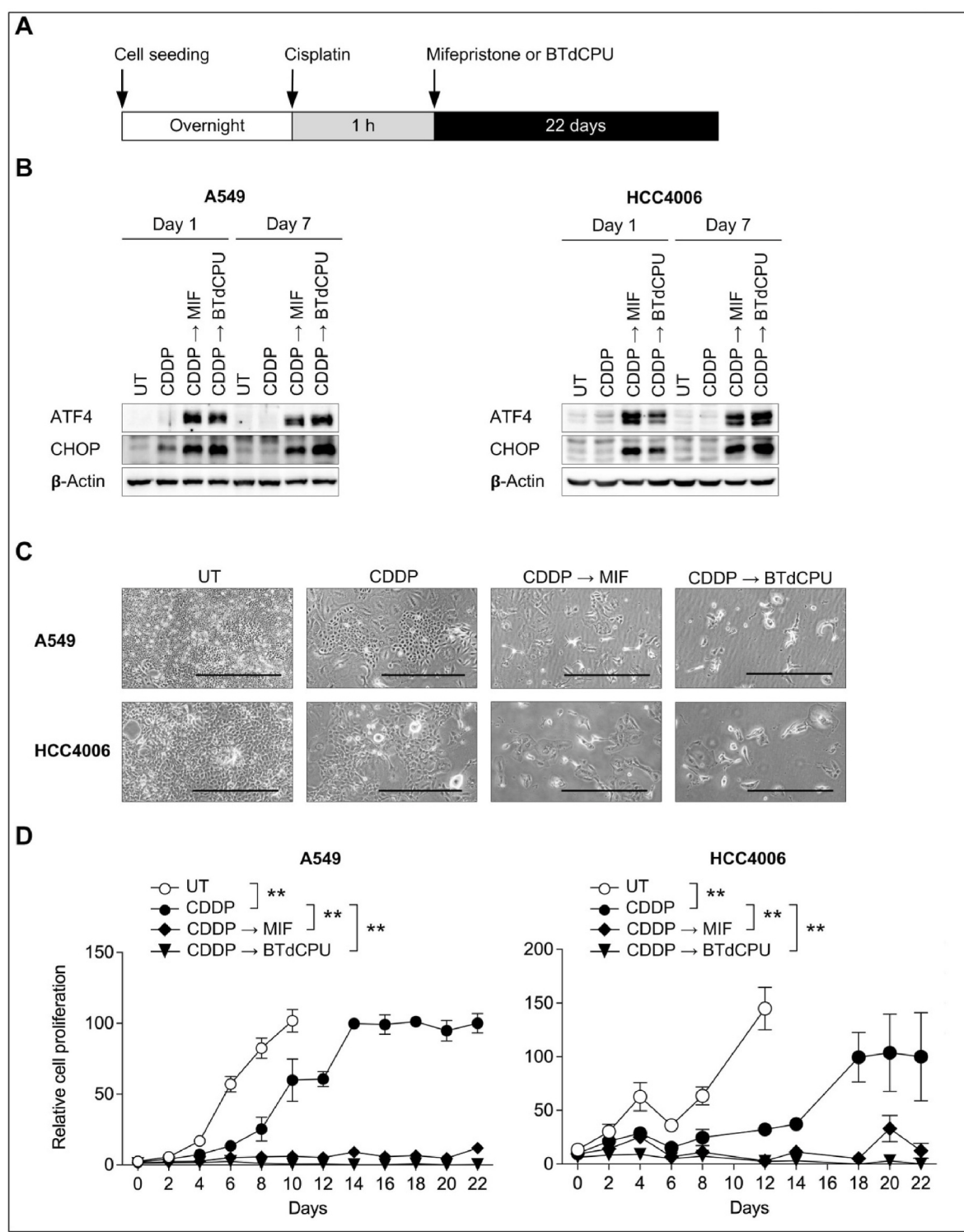


Fig. 7. Activation of the HRI/eIF2 α /ATF4 axis inhibits NSCLC re-proliferation after cisplatin treatment.

(A) Schematic representation of NSCLC re-proliferation assay. (B) Representative immunoblots of ATF4 and CHOP in A549 and HCC4006 cells treated with 100 μ M cisplatin (CDDP) followed by 20 μ M mifepristone (MIF) or 5 μ M BTdCPU for the indicated time periods. (C) Representative microscopic images of A549 cells treated with cisplatin (CDDP) only or cisplatin followed by mifepristone or BTdCPU for 8 days. Scale bars, 500 μ M. (D) Relative cell proliferation of A549 and HCC4006 cells determined by WST-8 assay. The indicated cells were pretreated with 100 μ M cisplatin for 1 h followed by 20 μ M mifepristone (MIF) or 5 μ M BTdCPU for 22 days. Data are means \pm SEMs ($n = 4$). Statistical analysis was performed by two-ANOVA, ** $p < 0.01$. Data are representative of three reproducible and independent experiments.

mediated by Akt. We examined the expression of TRIB3, a marker of this anti-survival signal in ISR-induced apoptosis and found that mifepristone enhanced the cisplatin-induced increase in TRIB3 in both cell lines (Fig. 8D and Supplementary Fig. S7).

The extrinsic pathway of apoptosis involves the formation of a death-inducing signaling complex (DISC) upon activation of cell surface receptors, leading to caspase activation. In the context of ISR-induced apoptosis, Death Receptor 5 (DR5) is a known marker. Mifepristone

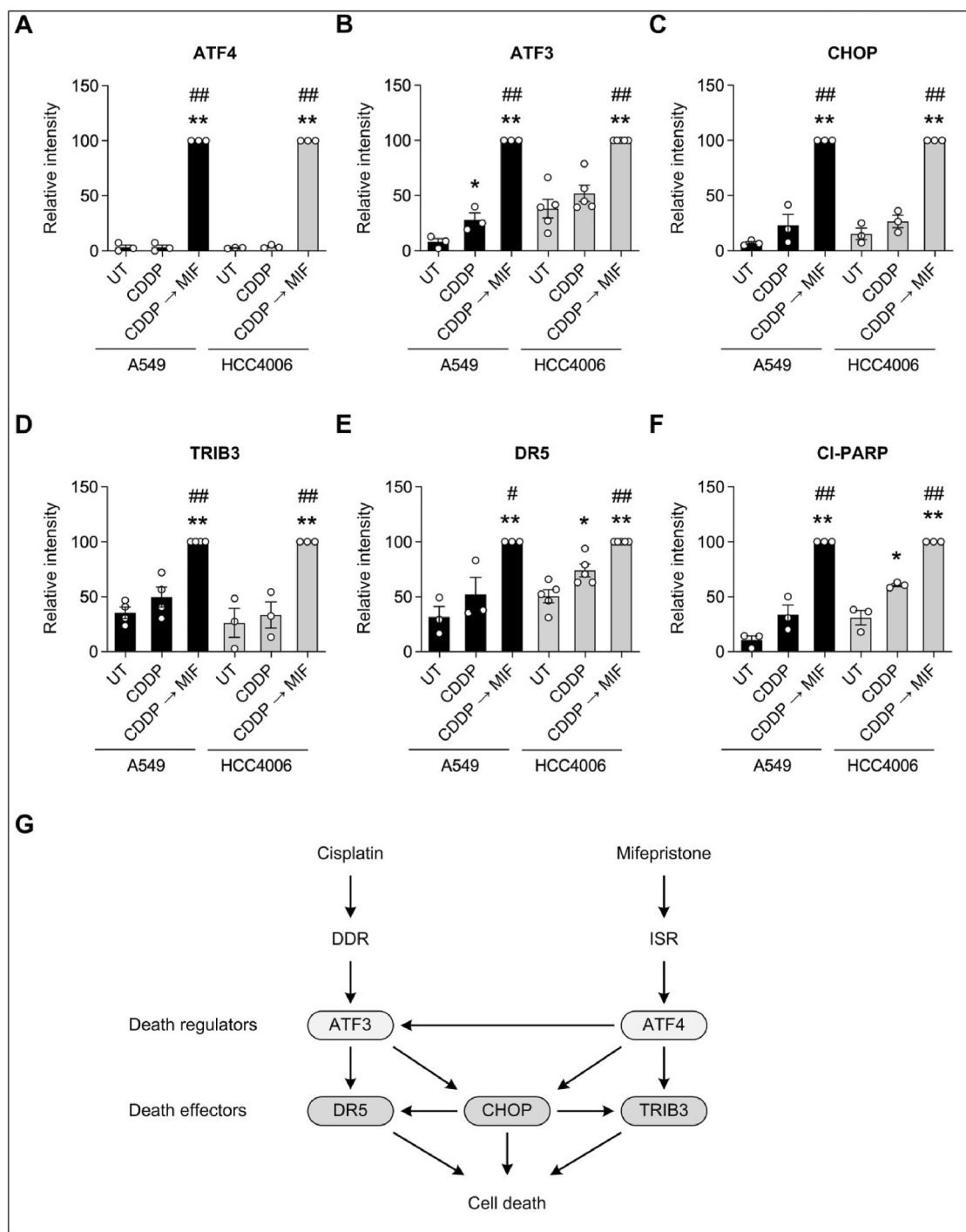


Fig. 8. Mifepristone inhibits NSCLC re-proliferation after cisplatin treatment through ISR-mediated cell death.

(A) The expression of ATF4 in A549 and HCC4006 cells treated with either cisplatin only or cisplatin followed by mifepristone for 6 h (n = 3). (B) The expression of ATF3 in A549 and HCC4006 cells treated with either cisplatin only or cisplatin followed by mifepristone for 12 h (n = 3–5). (C) The expression of pro-apoptotic protein CHOP in A549 and HCC4006 cells treated with either cisplatin only or cisplatin followed by mifepristone for 24 h (n = 3). (D) The expression of pro-apoptotic protein TRIB3 in A549 and HCC4006 cells treated with either cisplatin only or cisplatin followed by mifepristone for 24 h (n = 3–4). (E) The expression of pro-apoptotic protein DR5 in A549 and HCC4006 cells treated with either cisplatin only or cisplatin followed by mifepristone for 48 h (n = 3–5). (F) The expression of apoptotic marker CI-PARP in A549 and HCC4006 cells treated with either cisplatin only or cisplatin followed by mifepristone for 48 h (n = 3). Statistical analysis was performed by Student's t-test, *p < 0.05, **p < 0.01 compared to UT and #p < 0.05, ##p < 0.01 compared to CDDP. (G) Schematic depiction of the mechanism of action mifepristone as a cisplatin chemosensitizer for NSCLC. Cisplatin activates the DNA damage response (DDR), leading to the induction of the death regulator ATF3. ATF3, in turn, transcriptionally induces death effectors such as DR5 and CHOP. On the other hand, mifepristone activates the Integrated Stress Response (ISR), leading to the induction of the death regulator ATF4. ATF4 then transcriptionally induces death effectors TRIB3 and CHOP, and further amplifies the induction of these death effectors through the induction of ATF3 and CHOP. In sum, mifepristone has the potential to enhance the anti-cancer effects of cisplatin, underscoring its potential role as a chemosensitizer in cancer therapy.

enhanced the cisplatin-induced increase in DR5 in both A549 and HCC4006 cells (Fig. 8E and Supplementary Fig. S7). These results suggest that both intrinsic and extrinsic pathways of apoptosis contribute to the cell death of NSCLC cell lines enhanced by mifepristone.

Among death regulators of the ISR, the transcription factors ATF4 and ATF3 are known to coordinately induce these death effectors in the intrinsic and extrinsic pathways of apoptosis. As expected, mifepristone enhanced the cisplatin-induced induction of both ATF4 and ATF3 in both cell lines (Fig. 8A and B and Supplementary Fig. S7). In summary, our results indicate that mifepristone enhances the anti-tumor effects of cisplatin not only through tumor growth inhibition but also through ISR-mediated apoptosis induction in NSCLC.

4. Discussion

Cisplatin resistance poses a significant challenge in NSCLC, often leading to tumor recurrence and metastasis. Hence, identifying cisplatin chemosensitizers is a promising therapeutic strategy. Our drug repositioning approach, based on ISR activator screening, pinpointed mifepristone as a compound with potential chemosensitizing effects on cisplatin.

Mifepristone monotherapy has been documented to enhance both the lifespan and quality of life in murine models of spontaneous breast cancer [21], leukemia [22], lung cancer [23], and testicular and prostate cancer [24]. Historically, the anti-tumor properties of mifepristone have been ascribed to its action on the progesterone receptor-dependent pathway, especially in the context of breast cancer. For instance, over-expression of progesterone receptors, as reported in BRCA1 mutated mammary epithelial cells, has been implicated in explaining the anti-tumorigenic effects of mifepristone [21]. However, the expression of progesterone receptors has been linked to a favorable prognosis in breast cancer patients [25]. Furthermore, several studies have demonstrated the ability of mifepristone to inhibit the proliferation of gastric [26], prostate [27], and lung [28] cancer cells lacking progesterone receptors. This has led to a debate regarding the role of this pathway in the etiology of breast cancer. In concordance with our findings, it has been reported that the anti-tumor efficacy of mifepristone is augmented when mifepristone is administered subsequent to cisplatin treatment in ovarian cancer cells [29]. Thus, the chemosensitizing effects of mifepristone on cisplatin, mediated via ISR as identified in our study, may potentially contribute to its anti-cancer effects in malignancies beyond lung cancer.

The ISR and UPR are interconnected in PERK activation triggered by ER stress, and can induce ATF4, a vital mediator of the ISR. Some reports suggesting that mifepristone induces ATF4 through ER stress rather than the ISR [30–32]. Zhang et al. have previously demonstrated that mifepristone induces ER stress because of increased mRNA translation rate in ovarian cancer cells [30]. However, in our experiments, we did not detect an increase in mRNA translation in MEF cells treated with high doses of mifepristone; instead, we observed its inhibition (Supplementary Fig. S8). On the other hand, mifepristone has been reported that activates an atypical UPR that does not activate all three branches of the UPR in A549 cells and ovarian cancer cell lines, respectively [31,32]. However, in our hands, we did not find any evidence of UPR activation in MEF cells treated with mifepristone (Supplementary Fig. S9). The discrepancies between our results and previous studies concerning the involvement of ER stress may be attributable to issues with the detection sensitivity of UPR activation. Even in eIF2 $\alpha^{A/A}$ cells where ISR is absent, a slight induction of ATF4 is observed, indicating that mifepristone can induce ATF4 through pathways other than the ISR. However, based on the results presented in Fig. 3A, we posit that the contribution of non-ISR pathways to ATF4 induction by mifepristone is considerably minor compared to that of ISR.

The targeting of ISR in cancer treatment has recently gained attention because inducing the ISR can selectively tip the balance of cancer cells towards apoptosis [7]. Indeed, we have previously reported that

atovaquone, an FDA-approved antimicrobial, has anti-cancer activity in acute myeloid leukemia by activating the ISR through ATF4 induction [33]. The cell death mechanism by ISR activation has been widely studied, and CHOP has been most extensively validated as a cell death effector in therapy-induced cell death [34,35]. The transcription factor CHOP induces various pro-apoptotic factors such as DR5 [36], TRIB3 [37], BH3-only protein BIM [38], PUMA [39], and suppresses the expression of the anti-apoptotic protein BCL-2 [40]. On the other hand, the expression of ATF3 is reported to increase not only by ISR but also by DNA damage such as cisplatin [41], and we were also able to confirm that ATF4 was not induced by cisplatin, but ATF3 was. ATF3 is induced by ATF4 and forms a complex with ATF4 to transcriptionally activate CHOP [42]. The induction of DR5 is regulated by the ATF4-CHOP axis [36], and it has been reported that ATF4 and CHOP cooperate to transcriptionally activate TRIB3 [37]. These cell death signal transduction cascades are consistent with the molecular mechanism of apoptosis enhanced by mifepristone (Fig. 8G). While the involvement of apoptosis is unequivocal, we cannot rule out the possibility that other forms of cell death may also contribute. Further detailed analyses of cell death mechanisms remain a subject for future investigation.

On the other hand, the molecular mechanism of HRI activation by mifepristone has not been elucidated in this study. We and other researchers have previously demonstrated that HRI activation can be induced by reactive oxygen species production [43,44]. Therefore, it is possible that mifepristone induces reactive oxygen species production, leading to HRI activation. This is particularly interesting because resistance to cisplatin has been shown to be mediated by increasing the expression of antioxidant systems for survival [45–47]. Compound-induced reactive oxygen species production has been shown to sensitize cancer cells to cisplatin and carboplatin [47]. In future research, we would like to tackle the remaining question of how mifepristone activates HRI.

This study provides strong evidence for the efficacy of targeting the ISR as a novel adjuvant therapy to enhance cisplatin chemotherapy and prevent tumor recurrence. Importantly, the dosage used in this study was 60 mg/kg/day, which exceeds the dosages previously administered in human cancer patient case studies; therefore, further investigations into the therapeutic effective concentration are warranted. Given the widespread use of mifepristone in reproductive medicine and endocrine disorders, its safety and pharmacokinetics are well-studied [48,49], making it easier to progress to clinical trials. We look forward to the evaluation of the effectiveness of mifepristone against NSCLC after cisplatin treatment in a future clinical trial.

CRediT authorship contribution statement

Jirapat Namkaew: Writing – original draft, Validation, Investigation, Formal analysis. **Jun Zhang:** Validation, Investigation, Formal analysis. **Norio Yamakawa:** Validation, Investigation, Formal analysis. **Yoshimasa Hamada:** Methodology. **Kazue Tsugawa:** Validation. **Miho Oyadomari:** Methodology. **Masato Miyake:** Methodology. **Toyomasa Katagiri:** Supervision, Resources. **Seiichi Oyadomari:** Writing – review & editing, Writing – original draft, Supervision, Resources, Project administration, Funding acquisition, Conceptualization.

Declaration of competing interest

The authors declare that they have no known competing financial interests or personal relationships that could have appeared to influence the work reported in this paper.

Acknowledgments

This work is a result of collaborative research with Taiho Pharmaceutical and was supported by JSPS KAKENHI Grant Number 19H02853 to SO and Joint Usage and Joint Research Programs, the Institute of

Advanced Medical Sciences, Tokushima University.

Appendix A Supplementary data

Supplementary data to this article can be found online at <https://doi.org/10.1016/j.canlet.2023.216509>.

References

- [1] L.A. Torre, F. Bray, R.L. Siegel, J. Ferlay, J. Lortet-Tieulent, A. Jemal, Global cancer statistics, 2012, CA Cancer J Clin 65 (2015) 87–108.
- [2] J.R. Molina, P. Yang, S.D. Cassivi, S.E. Schild, A.A. Adjei, Non-small cell lung cancer: epidemiology, risk factors, treatment, and survivorship, Mayo Clin. Proc. 83 (2008) 584–594.
- [3] J.H. Schiller, D. Harrington, C.P. Belani, C. Langer, A. Sandler, J. Krook, J. Zhu, D. H. Johnson, G. Eastern Cooperative Oncology, Comparison of four chemotherapy regimens for advanced non-small-cell lung cancer, N. Engl. J. Med. 346 (2002) 92–98.
- [4] Y. Ohe, Y. Ohashi, K. Kubota, T. Tamura, K. Nakagawa, S. Negoro, Y. Nishiwaki, N. Saito, Y. Ariyoshi, M. Fukuoka, Randomized phase III study of cisplatin plus irinotecan versus carboplatin plus paclitaxel, cisplatin plus gemcitabine, and cisplatin plus vinorelbine for advanced non-small-cell lung cancer: four-Arm Cooperative Study in Japan, Ann. Oncol. 18 (2007) 317–323.
- [5] R. Arriagada, B. Bergman, A. Dunant, T. Le Chevalier, J.P. Pignon, J. Vansteenkiste, G. International, Adjuvant Lung Cancer Trial Collaborative, Cisplatin-based adjuvant chemotherapy in patients with completely resected non-small-cell lung cancer, N. Engl. J. Med. 350 (2004) 351–360.
- [6] J.P. Pignon, H. Tribodet, G.V. Scagliotti, J.Y. Douillard, F.A. Shepherd, R. J. Stephens, A. Dunant, V. Torri, R. Rossell, L. Seymour, S.G. Spiro, E. Rolland, R. Fossati, D. Aubert, K. Ding, D. Waller, T. Le Chevalier, L.C. Group, Lung adjuvant cisplatin evaluation: a pooled analysis by the LACE Collaborative Group, J. Clin. Oncol. 26 (2008) 3552–3559.
- [7] M. Costa-Mattioli, P. Walter, The integrated stress response: from mechanism to disease, Science 368 (2020).
- [8] K.M. Vattem, R.C. Wek, Reinitiation involving upstream ORFs regulates ATF4 mRNA translation in mammalian cells, Proc. Natl. Acad. Sci. U.S.A. 101 (2004) 11269–11274.
- [9] P.D. Lu, H.P. Harding, D. Ron, Translation reinitiation at alternative open reading frames regulates gene expression in an integrated stress response, J. Cell Biol. 167 (2004) 27–33.
- [10] I.M.N. Wortel, L.T. van der Meer, M.S. Kilberg, F.N. van Leeuwen, Surviving stress: modulation of ATF4-mediated stress responses in normal and malignant cells, Trends Endocrinol. Metabol. 28 (2017) 794–806.
- [11] S. Oyadomari, M. Mori, Roles of CHOP/GADD153 in endoplasmic reticulum stress, Cell Death Differ. 11 (2004) 381–389.
- [12] M.R. Thompson, D. Xu, B.R. Williams, ATF3 transcription factor and its emerging roles in immunity and cancer, J. Mol. Med. (Berl.) 87 (2009) 1053–1060.
- [13] M. Salazar, M. Lorente, A. Orea-Soufi, D. Davila, T. Erazo, J. Lizcano, A. Carracedo, E. Kiss-Toth, G. Velasco, Oncosuppressive functions of tribbles pseudokinase 3, Biochem. Soc. Trans. 43 (2015) 1122–1126.
- [14] C. Darini, N. Ghaddar, C. Chabot, G. Assaker, S. Sabri, S. Wang, J. Krishnamoorthy, M. Buchanan, A. Aguilar-Mahecha, B. Abdulkarim, J. Deschenes, J. Torres, J. Ursini-Siegel, M. Basik, A.E. Koromilas, An integrated stress response via PKR suppresses HER2+ cancers and improves trastuzumab therapy, Nat. Commun. 10 (2019) 2139.
- [15] M. Miyake, A. Nomura, A. Ogura, K. Takehana, Y. Kitahara, K. Takahara, K. Tsugawa, C. Miyamoto, N. Miura, R. Sato, K. Kurahashi, H.P. Harding, M. Oyadomari, D. Ron, S. Oyadomari, Skeletal muscle-specific eukaryotic translation initiation factor 2alpha phosphorylation controls amino acid metabolism and fibroblast growth factor 21-mediated non-cell-autonomous energy metabolism, FASEB J 30 (2016) 798–812.
- [16] I. Novoa, H. Zeng, H.P. Harding, D. Ron, Feedback inhibition of the unfolded protein response by GADD34-mediated dephosphorylation of eIF2alpha, J. Cell Biol. 153 (2001) 1011–1022.
- [17] S. Dey, T.D. Baird, D. Zhou, L.R. Palam, D.F. Spandau, R.C. Wek, Both transcriptional regulation and translational control of ATF4 are central to the integrated stress response, J. Biol. Chem. 285 (2010) 33165–33174.
- [18] K. Ameri, A.L. Harris, Activating transcription factor 4, Int. J. Biochem. Cell Biol. 40 (2008) 14–21.
- [19] S. Taniguchi, M. Miyake, K. Tsugawa, M. Oyadomari, S. Oyadomari, Integrated stress response of vertebrates is regulated by four eIF2alpha kinases, Sci. Rep. 6 (2016), 32886.
- [20] T. Chen, D. Ozel, Y. Qiao, F. Harbinski, L. Chen, S. Denoyelle, X. He, N. Zvereva, J. G. Supko, M. Chorev, J.A. Halperin, B.H. Aktas, Chemical genetics identify eIF2alpha kinase heme-regulated inhibitor as an anticancer target, Nat. Chem. Biol. 7 (2011) 610–616.
- [21] A.J. Poole, Y. Li, Y. Kim, S.C. Lin, W.H. Lee, E.Y. Lee, Prevention of Brca1-mediated mammary tumorigenesis in mice by a progesterone antagonist, Science 314 (2006) 1467–1470.
- [22] J.H. Check, L. Sansoucie, J. Chern, N. Amadi, Y. Katz, Mifepristone treatment improves length and quality of survival of mice with spontaneous leukemia, Anticancer Res. 29 (2009) 2977–2980.
- [23] J.H. Check, L. Sansoucie, J. Chern, E. Dix, Mifepristone treatment improves length and quality of survival of mice with spontaneous lung cancer, Anticancer Res. 30 (2010) 119–122.
- [24] J.H. Check, E. Dix, C. Wilson, D. Check, Progesterone receptor antagonist therapy has therapeutic potential even in cancer restricted to males as evidenced from murine testicular and prostate cancer studies, Anticancer Res. 30 (2010) 4921–4923.
- [25] V.J. Bardou, G. Arpino, R.M. Elledge, C.K. Osborne, G.M. Clark, Progesterone receptor status significantly improves outcome prediction over estrogen receptor status alone for adjuvant endocrine therapy in two large breast cancer databases, J. Clin. Oncol. 21 (2003) 1973–1979.
- [26] D.Q. Li, Z.B. Wang, J. Bai, J. Zhao, Y. Wang, K. Hu, Y.H. Du, Effects of mifepristone on proliferation of human gastric adenocarcinoma cell line SGC-7901 in vitro, World J. Gastroenterol. 10 (2004) 2628–2631.
- [27] M.F. El Etreby, Y. Liang, M.H. Johnson, R.W. Lewis, Antitumor activity of mifepristone in the human LNCaP, LNCaP-C4, and LNCaP-C4-2 prostate cancer models in nude mice, Prostate 42 (2000) 99–106.
- [28] H.E. Kapperman, A.A. Goyeneche, C.M. Telleria, Mifepristone inhibits non-small cell lung carcinoma cellular escape from DNA damaging cisplatin, Cancer Cell Int. 18 (2018) 185.
- [29] E.M. Freeburg, A.A. Goyeneche, C.M. Telleria, Mifepristone abrogates repopulation of ovarian cancer cells in between courses of cisplatin treatment, Int. J. Oncol. 34 (2009) 743–755.
- [30] L. Zhang, M.B. Hapon, A.A. Goyeneche, R. Srinivasan, C.D. Gamarra-Luques, E. A. Callegari, D.D. Drappeau, E.J. Terpstra, B. Pan, J.R. Knapp, J. Chien, X. Wang, K. M. Eyster, C.M. Telleria, Mifepristone increases mRNA translation rate, triggers the unfolded protein response, increases autophagic flux, and kills ovarian cancer cells in combination with proteasome or lysosome inhibitors, Mol. Oncol. 10 (2016) 1099–1117.
- [31] N. Dioufa, E. Kassi, A.G. Papavassiliou, H. Kiaris, Atypical induction of the unfolded protein response by mifepristone, Endocrine 38 (2010) 167–173.
- [32] P. Bastola, G.S. Leiserowitz, J. Chien, Multiple components of protein homeostasis pathway can be targeted to produce drug synergies with VCP inhibitors in ovarian cancer, Cancers 14 (2022).
- [33] A.M. Stevens, M. Xiang, L.N. Heppler, I. Tosic, K. Jiang, J.O. Munoz, A.S. Gaikwad, T.M. Horton, X. Long, P. Narayanan, E.L. Seashore, M.C. Terrell, R. Rashid, M. J. Krueger, A.E. Mangubat-Medina, T.Z. Ball, P. Sumazin, S.R. Walker, Y. Hamada, S. Oyadomari, M.S. Redell, D.A. Frank, Atovaquone is active against AML by upregulating the integrated stress pathway and suppressing oxidative phosphorylation, Blood Adv 3 (2019) 4215–4227.
- [34] W. Wang, G. Oguz, P.L. Lee, Y. Bao, P. Wang, M.G. Terp, H.J. Ditzel, Q. Yu, KDM4B-regulated unfolded protein response as a therapeutic vulnerability in PTEN-deficient breast cancer, J. Exp. Med. 215 (2018) 2833–2849.
- [35] T. Narita, M. Ri, A. Masaki, F. Mori, A. Ito, S. Kusumoto, T. Ishida, H. Komatsu, S. Iida, Lower expression of activating transcription factors 3 and 4 correlates with shorter progression-free survival in multiple myeloma patients receiving bortezomib plus dexamethasone therapy, Blood Cancer J. 5 (2015) e373.
- [36] M. Lu, D.A. Lawrence, S. Marsters, D. Acosta-Alvear, P. Kimmig, A.S. Mendez, A. W. Paton, J.C. Paton, P. Walter, A. Ashkenazi, Opposing unfolded-protein-response signals converge on death receptor 5 to control apoptosis, Science 345 (2014) 98–101.
- [37] N. Ohoka, S. Yoshii, T. Hattori, K. Onozaki, H. Hayashi, TRB3, a novel ER stress-inducible gene, is induced via ATF4-CHOP pathway and is involved in cell death, EMBO J. 24 (2005) 1243–1255.
- [38] H. Puthalakath, L.A. O'Reilly, P. Gunn, L. Lee, P.N. Kelly, N.D. Huntington, P. D. Hughes, E.M. Michalak, J. McKimm-Breschkin, N. Motoyama, T. Gotoh, S. Akira, P. Bouillet, A. Strasser, ER stress triggers apoptosis by activating BH3-only protein Bim, Cell 129 (2007) 1337–1349.
- [39] J. Li, B. Lee, A.S. Lee, Endoplasmic reticulum stress-induced apoptosis: multiple pathways and activation of p53-up-regulated modulator of apoptosis (PUMA) and NOXA by p53, J. Biol. Chem. 281 (2006) 7260–7270.
- [40] K.D. McCullough, J.L. Martindale, L.O. Klotz, T.Y. Aw, N.J. Holbrook, Gadd153 sensitizes cells to endoplasmic reticulum stress by down-regulating Bcl2 and perturbing the cellular redox state, Mol. Cell Biol. 21 (2001) 1249–1259.
- [41] J. Bar, M.S. Hasim, T. Baghai, N. Niknejad, T.J. Perkins, D.J. Stewart, H.S. Sekhon, P.J. Villeneuve, J. Dimitroulakos, Induction of activating transcription factor 3 is associated with cisplatin responsiveness in non-small cell lung carcinoma cells, Neoplasia 18 (2016) 525–535.
- [42] H.Y. Jiang, S.A. Wek, B.C. McGrath, D. Lu, T. Hai, H.P. Harding, X. Wang, D. Ron, D.R. Cavener, R.C. Wek, Activating transcription factor 3 is integral to the eukaryotic initiation factor 2 kinase stress response, Mol. Cell Biol. 24 (2004) 1365–1377.
- [43] L. Lu, A.P. Han, J.J. Chen, Translation initiation control by heme-regulated eukaryotic initiation factor 2alpha kinase in erythroid cells under cytoplasmic stresses, Mol. Cell Biol. 21 (2001) 7971–7980.
- [44] Y. Hamada, Y. Furumoto, A. Izutani, S. Taniguchi, M. Miyake, M. Oyadomari, K. Teranishi, N. Shimomura, S. Oyadomari, Nanosecond pulsed electric fields induce the integrated stress response via reactive oxygen species-mediated heme-regulated inhibitor (HRI) activation, PLoS One 15 (2020), e0229948.
- [45] L. Galluzzi, L. Senovilla, I. Vitale, J. Michels, I. Martins, O. Kepp, M. Castedo, G. Kroemer, Molecular mechanisms of cisplatin resistance, Oncogene 31 (2012) 1869–1883.
- [46] C. Meijer, N.H. Mulder, H. Timmer-Bosscha, W.J. Sluiter, G.J. Meersma, E.G. de Vries, Relationship of cellular glutathione to the cytotoxicity and resistance of seven platinum compounds, Cancer Res. 52 (1992) 6885–6889.

- [47] J.T.T. Coates, G. Rodriguez-Berriguete, R. Puliyadi, T. Ashton, R. Prevo, A. Wing, G. Granata, G. Pirovano, G.W. McKenna, G.S. Higgins, The anti-malarial drug atovaquone potentiates platinum-mediated cancer cell death by increasing oxidative stress, *Cell Death Dis.* 6 (2020) 110.
- [48] C.M. Blassey, T.S. Block, J.K. Belanoff, R.L. Roe, Efficacy and safety of mifepristone for the treatment of psychotic depression, *J. Clin. Psychopharmacol.* 31 (2011) 436–440.
- [49] Y. Xiao, Y. Zhu, S. Yu, C. Yan, R.J. Ho, J. Liu, T. Li, J. Wang, L. Wan, X. Yang, H. Xu, J. Wang, X. Tu, L. Jia, Thirty-day rat toxicity study reveals reversible liver toxicity of mifepristone (RU486) and metapristone, *Toxicol. Mech. Methods* 26 (2016) 36–45.